Asymmetrical Grid Fault Ride-Through Strategy of Three-phase Grid-connected Inverter Considering Network Impedance Impact in Low Voltage Grid

Guo, Xiaoqiang; Zhang, Xue; Wang, Baocheng; Wu, Weiyang; Guerrero, Josep M.

Published in:
I E E E Transactions on Power Electronics

DOI (link to publication from Publisher):
10.1109/TPEL.2013.2278030

Publication date:
2014

Document Version
Early version, also known as pre-print

Asymmetrical Grid Fault Ride-Through Strategy of Three-phase Grid-connected Inverter Considering Network Impedance Impact in Low Voltage Grid

Xiaoqiang Guo, *Member, IEEE,* Xue Zhang, Baocheng Wang, Weiyang Wu, and Josep M. Guerrero, *Senior Member, IEEE*

Abstract—This paper presents a new control strategy of three-phase grid-connected inverter for the positive sequence voltage recovery and negative sequence voltage reduction under asymmetrical grid faults. Unlike the conventional control strategy based on an assumption that the network impedance is mainly inductive, the proposed control strategy is more flexible and effective by considering the network impedance impact, which is of great importance for the high penetration of grid-connected renewable energy systems into low-voltage grids. The experimental tests are carried out to validate the effectiveness of the proposed solution for the flexible voltage support in a low voltage grid, where the network impedance is mainly resistive.

Index Terms—Fault ride-through, grid faults, grid-connected inverter, flexible voltage support

X. Guo is with the Key Lab of Power Electronics for Energy Conservation and Motor drive of Hebei province, Department of Electrical Engineering, Yanshan University, Qinhuangdao 066004, China (e-mail: guoxq@ieee.org)

J. M. Guerrero is with the Department of Energy Technology, Aalborg University, Aalborg DK-9220, Denmark (e-mail: joz@et.aau.dk).

I. INTRODUCTION

With the high penetration of grid-connected renewable energy systems, the new grid codes or standards such as IEEE P1547.8 have been drafted [1], where the fault ride through (FRT) is a mandatory function. In order to meet the grid code requirements, a significant contribution made by Rodriguez, *et al* is the flexible power control concept [2], which facilitates multiple choices for FRT with different current references. Another interesting improvement was reported in [3], which achieved the flexible power quality regulation by considering the instantaneous power ripples and current harmonics. Other interesting solutions were reported recently [4-12], which enhanced the flexible operation of grid-connected Inverters under unbalanced grid faults. It should be noted that the above-mentioned control strategies mainly focus on the power control of grid-connected inverters, whereas the voltage support control of the positive sequence voltage recovery and negative sequence voltage reduction is not well explored. For the voltage support, Li, *et al* presented a power quality compensator to keep the microgrid voltage immune to unbalanced grid faults [13-14]. It is very effective but needs additional series compensation devices. In order to overcome the limitation, Camacho, *et al* presented a powerful voltage support control for the grid-connected inverter under unbalanced grid faults [15], which enables both the positive sequence voltage recovery and negative sequence voltage reduction. Indeed, it is valid on the assumption that the network impedance is mainly inductive. An interesting question might arise if the solution in [15] is still effective in case of the mainly resistive network impedance? The question is of great importance due to the high penetration of grid-connected systems in the low voltage grid, where the network impedance is mainly resistive [16-18].

The main contribution of this paper is to present a new FRT strategy of three-phase grid-connected inverter for the positive sequence voltage recovery and negative sequence voltage reduction by taking the network impedance impact into account. The experimental tests on a downscale prototype are carried out to

verify the effectiveness of the proposed solution in a low voltage grid.

II. PROPOSED VOLTAGE SUPPORT CONTROL

Fig.1 illustrates the block diagram of the grid-connected inverter. During grid faults, the network node voltage profile will deteriorate. In order to provide the voltage support function, the grid-connected inverter should inject the power into the network for improving the bus voltage profile.

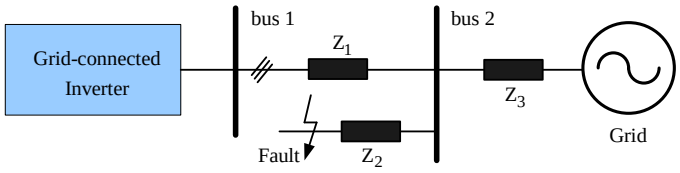

Fig.1. Block diagram of grid-connected inverter

The control diagram is shown in Fig.2, where $Z = R + jX$ is the equivalent aggregated network impedance seen from the bus1 to grid. A dc power supply is used to emulate the renewable energy resources and storage [19], for simplicity of analysis.

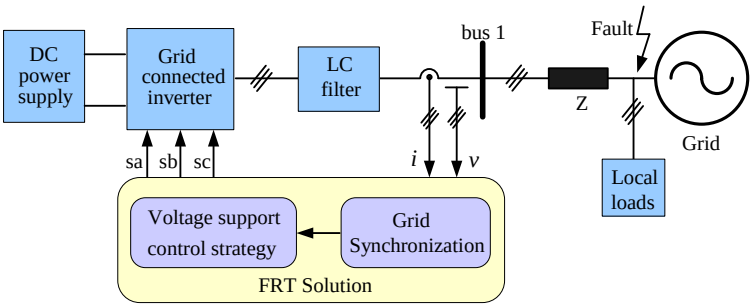

Fig.2. Control diagram of FRT solution for grid-connected inverter

The injected active and reactive power can be expressed in stationary reference frame as [20]

$$p = \frac{3}{2}\left(v_\alpha i_\alpha + v_\beta i_\beta\right) \tag{1}$$

$$q = \frac{3}{2}\left(v_\beta i_\alpha - v_\alpha i_\beta\right) \tag{2}$$

where v_α, v_β, i_α and i_β are the quadrature components of voltages and currents in the stationary reference frame, respectively.

For the conventional power control strategy, the active and reactive current can be derived from (1) and (2)

as follows:

$$\begin{bmatrix} i_{\alpha(p)} \\ i_{\beta(p)} \end{bmatrix} = \frac{2}{3}\frac{P^*}{v_\alpha^2 + v_\beta^2}\begin{bmatrix} v_\alpha \\ v_\beta \end{bmatrix} \tag{3}$$

$$\begin{bmatrix} i_{\alpha(q)} \\ i_{\beta(q)} \end{bmatrix} = \frac{2}{3}\frac{Q^*}{v_\alpha^2 + v_\beta^2}\begin{bmatrix} v_\beta \\ -v_\alpha \end{bmatrix} \tag{4}$$

where P^* and Q^* are the set points for the active and reactive power.

Under asymmetrical grid fault, equation (3) and (4) can be rewritten as follows [15].

$$\begin{bmatrix} i_{\alpha(p)} \\ i_{\beta(p)} \end{bmatrix} = \frac{2}{3}\frac{P^*}{D}\begin{bmatrix} v_\alpha^+ + v_\alpha^- \\ v_\beta^+ + v_\beta^- \end{bmatrix} \tag{5}$$

$$\begin{bmatrix} i_{\alpha(q)} \\ i_{\beta(q)} \end{bmatrix} = \frac{2}{3}\frac{Q^*}{D}\begin{bmatrix} v_\beta^+ + v_\beta^- \\ -v_\alpha^+ - v_\alpha^- \end{bmatrix} \tag{6}$$

where $D = \left(v_\alpha^+ + v_\alpha^-\right)^2 + \left(v_\beta^+ + v_\beta^-\right)^2 = \left(V^+\right)^2 + \left(V^-\right)^2 - 2\cos\left(2\omega t + \varphi_+ + \varphi_-\right)$, $v_\alpha^+ = V^+\sin\left(\omega t + \varphi_+\right)$, $v_\beta^+ = -V^+\cos\left(\omega t + \varphi_+\right)$, $v_\alpha^- = V^-\sin\left(\omega t + \varphi_-\right)$, $v_\beta^- = V^-\cos\left(\omega t + \varphi_-\right)$, $V^+ = \sqrt{\left(v_\alpha^+\right)^2 + \left(v_\beta^+\right)^2}$ and $V^- = \sqrt{\left(v_\alpha^-\right)^2 + \left(v_\beta^-\right)^2}$.

Note that the abovementioned objective is the instantaneous power control, which can achieve the constant power without oscillations. But it is not suitable for the voltage support under grid faults [15].

In order to achieve the flexible voltage support in case of different network impedances, a new control strategy is proposed by consider the relationship between the *R*/X ratio of the network impedance and voltage support as follows.

$$i_{\alpha(P)}^* = \frac{2}{3}P^*\frac{k^+v_\alpha^+ + \frac{R}{\sqrt{R^2+X^2}}\left(k^-v_\alpha^-\right)}{k^+\left(V^+\right)^2 + \frac{R}{\sqrt{R^2+X^2}}\left(k^-\left(V^-\right)^2\right)} \tag{7}$$

$$i_{\beta(P)}^* = \frac{2}{3}P^*\frac{k^+v_\beta^+ + \frac{R}{\sqrt{R^2+X^2}}\left(k^-v_\beta^-\right)}{k^+\left(V^+\right)^2 + \frac{R}{\sqrt{R^2+X^2}}\left(k^-\left(V^-\right)^2\right)} \tag{8}$$

$$i_{\alpha(Q)}^* = \frac{2}{3}Q^*\frac{k^+v_\beta^+ + \frac{X}{\sqrt{R^2+X^2}}\left(k^-v_\beta^-\right)}{k^+\left(V^+\right)^2 + \frac{X}{\sqrt{R^2+X^2}}\left(k^-\left(V^-\right)^2\right)} \tag{9}$$

$$i^*_{\beta(Q)}=\frac{2}{3}Q^*\frac{-k^+v^+_\alpha-\frac{X}{\sqrt{R^2+X^2}}\left(k^-v^-_\alpha\right)}{k^+\left(V^+\right)^2+\frac{X}{\sqrt{R^2+X^2}}\left(k^-\left(V^-\right)^2\right)} \tag{10}$$

Note that when the network impedance is mainly inductive，that is $\frac{R}{\sqrt{R^2+X^2}}\approx 0$ and $\frac{X}{\sqrt{R^2+X^2}}\approx 1$，equations (7)~(10) are exactly the same as (26), (27), (23) and (24) of the conventional control strategy [15]. However, for practical low-voltage grids, the network impedance is mainly resistive. Therefore, the proposed method could be greatly simplified by substituting $\frac{R}{\sqrt{R^2+X^2}}\approx 1$ and $\frac{X}{\sqrt{R^2+X^2}}\approx 0$ into (7)~(10) as follows.

$$i^*_{\alpha(P)}=\frac{2}{3}P^*\frac{k^+v^+_\alpha+\left(k^-v^-_\alpha\right)}{k^+\left(V^+\right)^2+\left(k^-\left(V^-\right)^2\right)} \tag{11}$$

$$i^*_{\beta(P)}=\frac{2}{3}P^*\frac{k^+v^+_\beta+\left(k^-v^-_\beta\right)}{k^+\left(V^+\right)^2+\left(k^-\left(V^-\right)^2\right)} \tag{12}$$

$$i^*_{\alpha(Q)}=\frac{2}{3}Q^*\frac{k^+v^+_\beta}{k^+\left(V^+\right)^2} \tag{13}$$

$$i^*_{\beta(Q)}=\frac{2}{3}Q^*\frac{-k^+v^+_\alpha}{k^+\left(V^+\right)^2} \tag{14}$$

Following will present a theoretical analysis of the proposed solution for the effective voltage support. The bus voltage in Fig.2 can be expressed as:

$$v_\alpha=v_{g\alpha}+Ri_\alpha+L\frac{di_\alpha}{dt} \tag{15}$$

$$v_\beta=v_{g\beta}+Ri_\beta+L\frac{di_\beta}{dt} \tag{16}$$

Substitute (11)~(14) into (15) and (16) with mathematical manipulations, the positive and negative sequence bus voltage amplitudes can be obtained.

$$V^+\approx V^+_g+\frac{2}{3}P^*\frac{RV^+k^+}{k^+\left(V^+\right)^2+k^-\left(V^-\right)^2} \tag{17}$$

$$V^-\approx V^-_g+\frac{2}{3}P^*\frac{RV^-k^-}{k^+\left(V^+\right)^2+k^-\left(V^-\right)^2} \tag{18}$$

Equation (17) and (18) indicate that the conventional method in [15] is not effective for the voltage support in the low voltage grid. On the other hand, the proposed method can achieve more effective voltage

support for the positive sequence voltage recovery and negative sequence voltage reduction in the low voltage grid. Following will present the system control strategy and experimental verification.

III. EXPERIMENTAL RESULTS

This section will present the effectiveness of the proposed voltage support strategy under grid fault in the low voltage grid, where the network impedance is mainly resistive. A DC Power source is used to emulate the renewable energy sources and storage. A Programmable AC source (Chroma 6590) is used to emulate the grid fault, whose voltage profiles are $v_{ga}=1\angle 0^{\circ}$, $v_{gb}=0.6837\angle -137^{\circ}$, $v_{gc}=0.6837\angle 137^{\circ}$, $V^{+}=0.7692$ and $V^{-}=0.2308$. The experimental system parameters are listed as follows. DC-link voltage is 150V, Rated grid voltage is 60V/50Hz, network impedance is 2+j0.3Ω, ant the inverter filter inductor and capacitor are 5mH and 9.9μF respectively.

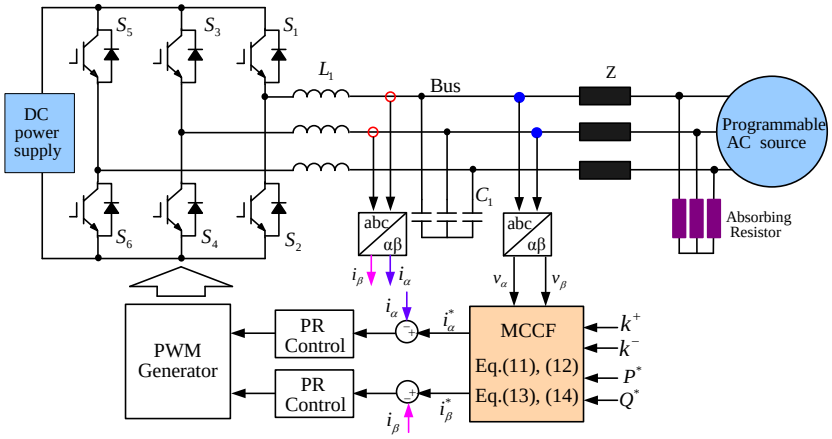

Fig.3. Block diagram of grid-connected inverter control

The block diagram of the system control structure is shown in Fig.3, where the positive and negative sequence voltages are estimated with MCCF-PLL [21]. The PR control is used for the grid current regulation [6]. Following will provide the experimental tests of the conventional and proposed control strategies for the flexible voltage support under grid faults. The test parameters are shown in Table 1.

TABLE I

TEST PARAMETERS

	Conventional Control (Test1)		Proposed Control (Test2)		Coefficient
Time/s	P^*	Q^*	P^*	Q^*	k^+
0~0.1	100W	0	100W	0	1
0.1~0.2	100W	0	100W	0	1
0.2~0.3	100W	150Var	250W	0	0.9
0.3~0.4	100W	150Var	250W	0	0.5
0.4~0.5	100 W	150Var	250 W	0	0.1

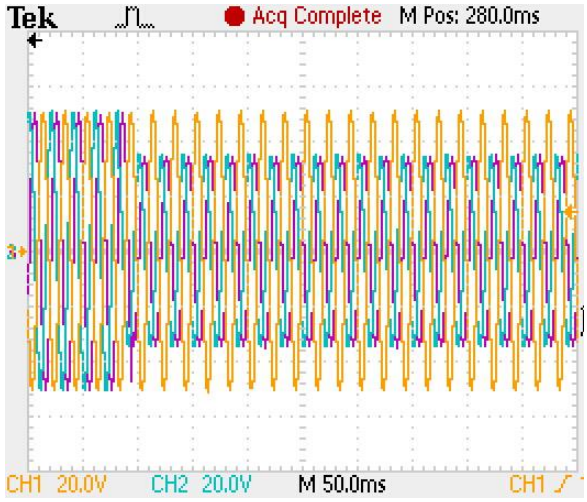

(a)

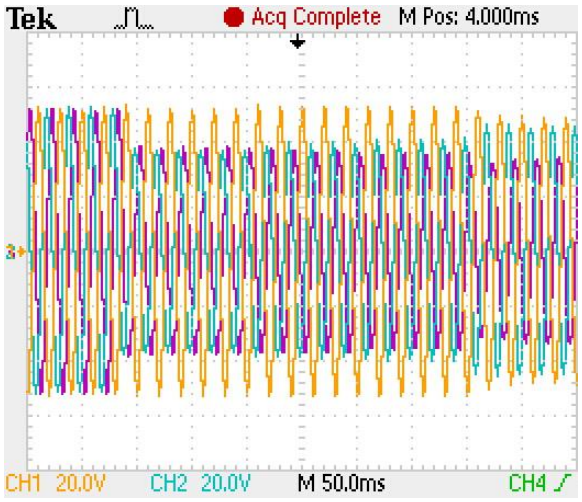

(b)

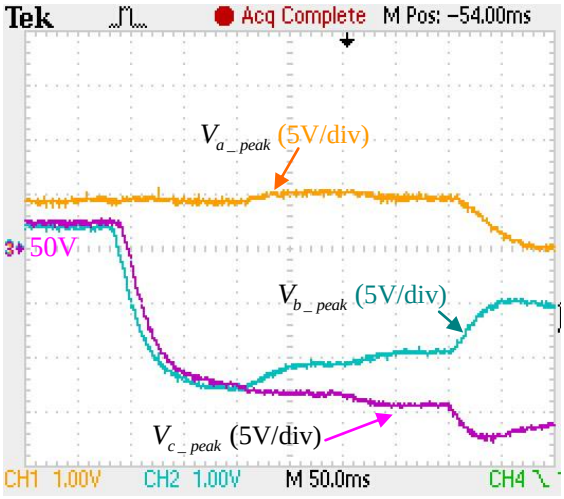

(c)

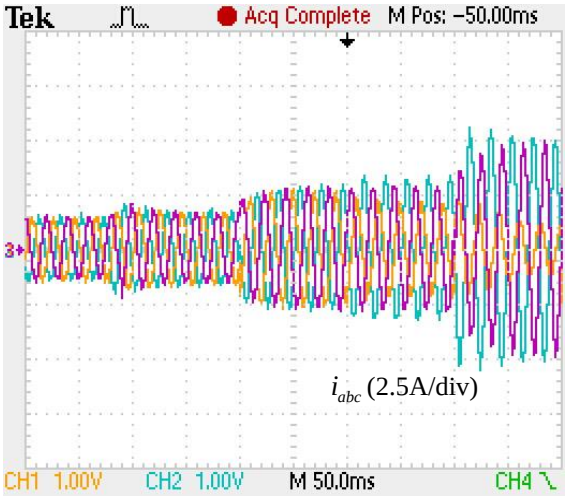

(d)

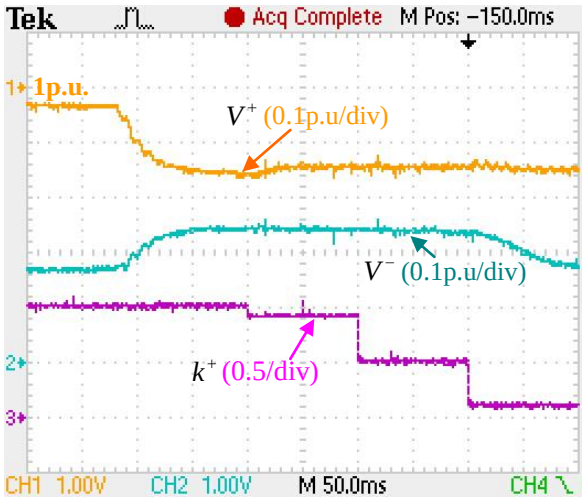

(e)

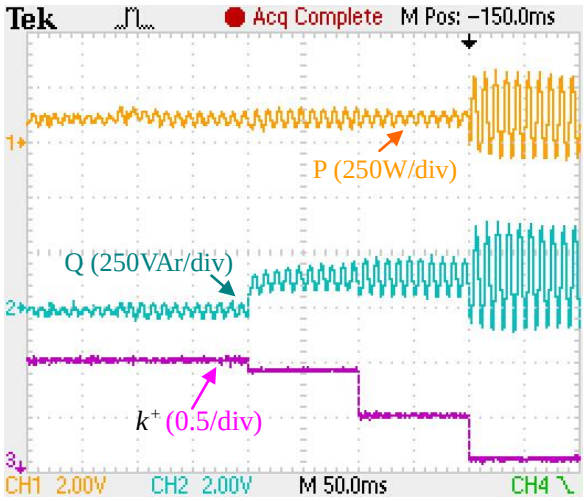

(f)

Fig.4 Experiment result of conventional solution (a) Emulated grid voltage. (b) Bus voltage. (c) Peak voltage of each phase. (d) Inverter current, (e) Positive/negative sequence voltage amplitude and coefficient 'k^+'. (f) Active/reactive power and coefficient 'k^+'

The experimental results of conventional solution are shown in Fig.4. The grid fault occurs at 0.1s, and the unbalanced voltage sag arises, as shown in Fig. 4(a) and (b). During 0.1 to 0.2s, no reactive power is injected. Three-phase voltage remains unchanged after the grid fault. During 0.2 to 0.3s, the control strategy with the reactive power injection is configured, as shown in Fig. 4(d) and (f). In agreement with the analysis of Section II, the experimental results in Fig.4 (b) indicate that the voltage support is not significantly enabled, which is different from the results in case of the inductive network impedance [15]. During 0.3 to 0.4s, $k^+ = k^- = 0.5$, the coordinate control of the positive and negative sequence voltages are configured. From Fig. 4(b), it can be observed that the voltage profile slightly changes. In this case, the current tends to be unbalanced for the negative sequence voltage reduction, as shown in Fig. 4(d). In order to minimize the negative sequence voltage, $k^+ = 0.9$ and $k^- = 0.1$ are configured during 0.4 to 0.5s. It can be observed that the unbalance degree of the bus voltage is mitigated, but still in a relatively high level, which is in agreement with the theoretical analysis in Section II.

In summary, the above results indicate that the voltage support with the conventional control strategy may work, but not be in an effective way, as previously discussed in Section II.

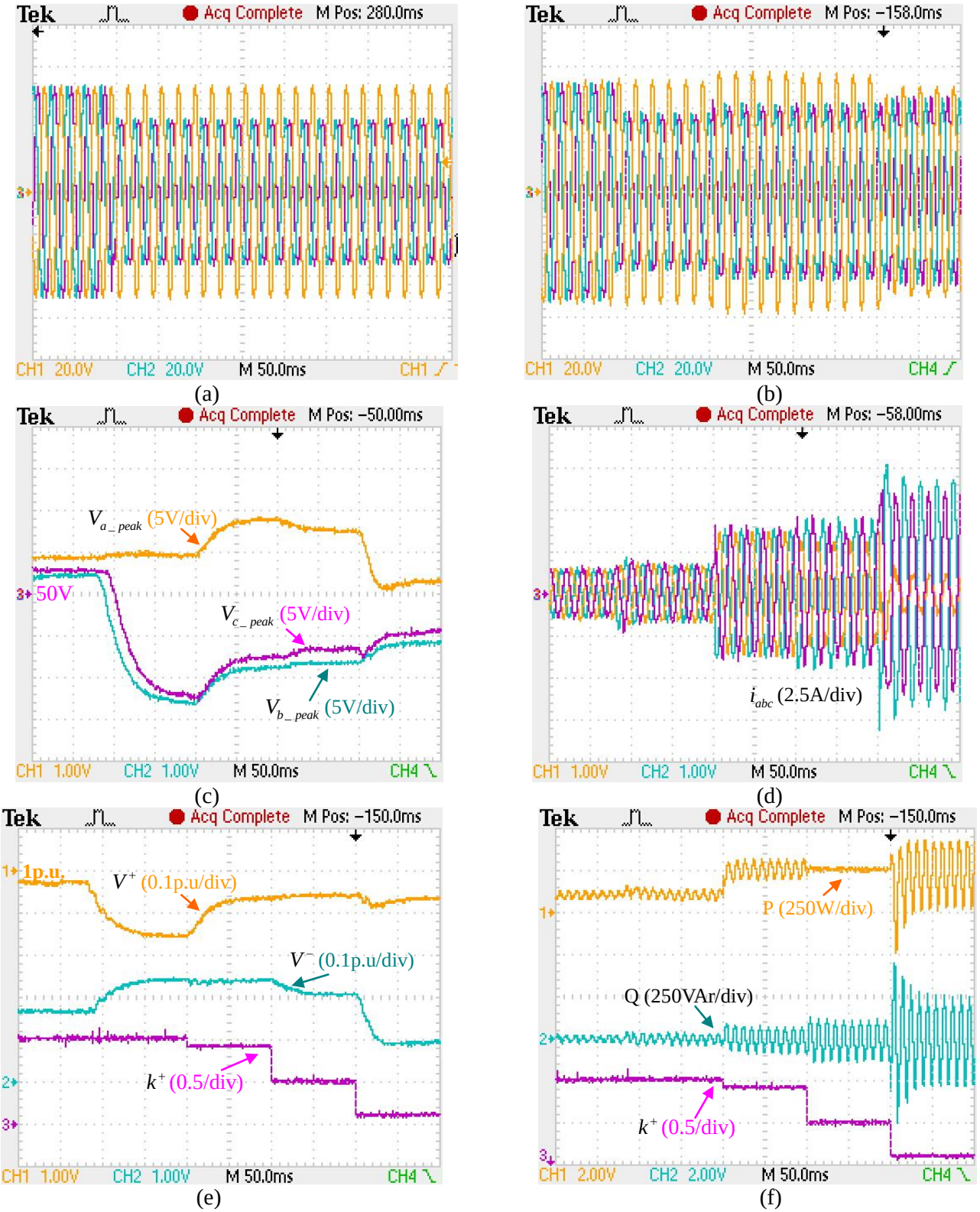

Fig.5 Experiment result of proposed solution (a) Emulated grid voltage. (b) Bus voltage. (c) Peak voltage of each phase. (d) Inverter current, (e) Positive/negative sequence voltage amplitude and coefficient 'k^+'. (f) Active/reactive power and coefficient 'k^+'

Fig.5 shows the experiment results of proposed solution. The grid fault occurs at 0.1s, and the unbalanced

voltage sag arises, as shown in Fig. 5(a) and (b). During 0.1 to 0.2s, no reactive power is injected. Three-phase voltage remains unchanged after the grid fault. During 0.2 to 0.3s, the proposed control strategy is enabled with $k^+ = 0.9$ and $k^- = -0.1$.In agreement with the analysis of Section II, the experimental results in Fig.5 indicate that the voltage support is significantly enhanced. During 0.3 to 0.4s, $k^+ = 0.5$ and $k^- = -0.5$, the coordinate control of the positive and negative sequence voltages are configured. From Fig.5, it can be observed that a tradeoff between positive sequence voltage support and negative sequence voltage reduction is achieved. In order to minimize the negative sequence voltage, $k^+ = 0.1$ and $k^- = -0.9$ are configured during 0.4 to 0.5s. It can be observed that the unbalance degree of the bus voltage is significantly decreased at the expense of the larger power oscillations, which would result in the dc-link voltage oscillations. Therefore, the control coefficient should be carefully tuned for the practical applications, and the systematic and optimized tuning method would be reported in our future paper.

In order to highlight the effectiveness of the proposed solution, a performance comparison between the conventional and proposed control strategy is presented in Fig.6. It is clear that the voltage support may work with the conventional solution, but not be in an effective way. On the other hand, the proposed control strategy is effective for both positive sequence voltage recovery and negative sequence voltage reduction, which will enhance the FRT capability of the grid-connected inverter in the low voltage grid.

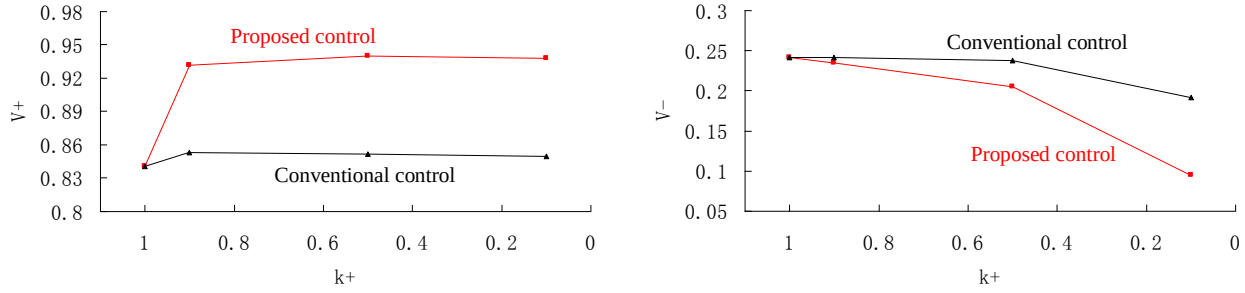

(a) (b)

Fig.6. Performance comparison between conventional and proposed solution. (a) Positive sequence voltage recovery. (b) Negative sequence voltage reduction.

V. CONCLUSIONS

In this paper, a new FRT control strategy of three-phase grid-connected inverter has been presented and evaluated through theoretical analysis and experimental tests. The obtained results indicate that the conventional FRT control strategy is not effective in the low voltage grid, where the network impedance is mainly resistive. On the other hand, the presented method can achieve the more effective voltage support with the positive sequence voltage recovery and negative sequence voltage reduction. It is expected that the presented solution will enhance the FRT capability for high penetration of grid-connected renewable energy system into the low voltage grid.

REFERENCE

[1] M. H. Coddington, B. D. Kroposki, and T. S. Basso, "Evaluating future standards and codes with a focus on high penetration photovoltaic (HPPV) system deployment," *in Proceedings of 35th IEEE Photovoltaic Specialists Conference* (*PVSC*), pp. 544–549, 2010

[2] P. Rodriguez, A. Timbus, R. Teodorescu, M. Liserre, and F. Blaabjerg, "Flexible active power control of distributed power generation systems during grid faults," *IEEE Trans. Ind. Electron.*, vol. 54, no. 5, pp. 2583–2592, Oct. 2007.

[3] M. Castilla, J. Miret, J. L. Sosa, J. Matas, and L. G. Vicuna, "Grid fault control scheme for three-phase photovoltaic inverters with adjustable power quality characteristics," *IEEE Trans. Power Electron.*, vol. 25, no. 12, pp. 2930–2940, Dec. 2010.

[4] P. Rodriguez, A. Timbus, R. Teodorescu, M. Liserre, and F. Blaabjerg, "Reactive power control for improving wind turbine system behavior under grid faults," *IEEE Trans. Power Electron.*, vol. 24, no. 7, pp. 1798–1801, Jul. 2009.

[5] I. Etxeberria-Otadui, U. Viscarret, M. Caballero, A. Rufer, and S. Bacha, "New optimized PWM VSC

control structures and strategies under unbalanced voltage transients," *IEEE Trans. Ind. Electron.*, vol. 54, no. 5, pp. 2902–2914, Oct. 2007.

[6] R. Teodorescu, M. Liserre, and P. Rodriguez, "Grid converters for photovoltaic and wind power systems," New York: IEEE Wiley, 2011.

[7] A. Junyent-Ferre, O. Gomis-Bellmunt, T.C. Green, and D.E. Soto-Sanchez, "Current control reference calculation issues for the operation of renewable source grid interface VSCs under unbalanced voltage sags," *IEEE Trans. Power Electron.*, vol. 26, no. 12, pp. 3744–3753, Dec. 2011.

[8] Y. A.-R. I. Mohamed, "Mitigation of dynamic, unbalanced, and harmonic voltage disturbances using grid-connected inverters with LCL filter," *IEEE Trans. Ind. Electron.*, vol. 58, no. 9, pp. 3914–3924, Sep. 2011.

[9] J. Miret, M. Castilla, A. Camacho, L. G. Vicuna, and J. Matas, "Control scheme for photovoltaic three-phase inverters to minimize peak currents during unbalanced grid-voltage sags," *IEEE Trans. Power Electron.*, vol. 27, no. 10, pp. 4262–4271, Oct. 2012.

[10] J. A. Suul, A. Luna, P. Rodriguez, and T. Undeland, "Virtual-flux-based voltage-sensor-less power control for unbalanced grid conditions," *IEEE Trans. Power Electron.*, vol. 27, no. 9, pp. 4071–4087, Jul. 2012.

[11] Z. R. Ivanovic, E. M.Adžić, M. S. Vekić, S. U. Grabić, N. L. Čelanović, and V. A. Katić, "HIL evaluation of power flow control strategies for energy storage connected to smart grid under unbalanced conditions," *IEEE Trans. Power Electron.*, vol. 27, no. 11, pp. 4699–4710, Nov. 2012.

[12] Changjin Liu, Dehong Xu, Nan Zhu, Frede Blaabjerg, and Min Chen, "DC-voltage fluctuation elimination through a DC-capacitor current control for DFIG converters under unbalanced grid voltage conditions," *IEEE Trans. Power Electron.*, vol. 28, no. 7, pp. 3206–3218, Jul. 2013.

[13] Y. Li, D. M. Vilathgamuwa, and P. C. Loh, "Microgrid power quality enhancement using a three-phase four-wire grid-interfacing compensator", *IEEE Trans. Ind. Appl.*, vol. 41, no. 6, pp. 1707-1719, Nov./Dec. 2005.

[14] Y. Li, D. M. Vilathgamuwa, and P. C. Loh, "A grid-interfacing power quality compensator for three-phase three-wire microgrid applications", *IEEE Trans. Power Electron.*, vol. 21, no. 4, pp. 1021-1031, Jul. 2006.

[15] A. Camacho, M. Castilla, J. Miret, J. Vasquez, and E. Alarcon-Gallo, "Flexible voltage support control for three phase distributed generation inverters under grid fault," *IEEE Trans. Ind. Electron.*, vol. 60, no. 4, pp. 1429–1441, Apr. 2013.

[16] J. M. Guerrero, J. Matas, L. García de Vicuña, M. Castilla, and J. Miret, "Decentralized control for parallel operation of distributed generation inverters using resistive output impedance," *IEEE Trans. Ind. Electron.*, vol. 54, no. 2, pp. 994–1004, Apr. 2007.

[17] T. L. Vandoorn, B. Meersman, L. Degroote, B. Renders, and L. Vandevelde, "A control strategy for islanded microgrids with dc-link voltage control," *IEEE Trans. Power Del*., vol. 26, no. 2, pp. 703–713, Apr. 2011.

[18] Q.-C. Zhong, "Robust droop controller for accurate proportional load sharing among inverters operated in parallel," *IEEE Trans. Ind. Electron*., vol. 60, no. 4, pp. 1281–1290, Apr. 2013.

[19] Y. Li and Y. W. Li, "Power management of inverter interfaced autonomous microgrid based on virtual frequency-voltage frame," *IEEE Trans on Smart Grid*, vol. 2, no. 3, pp. 30-40, Mar, 2011.

[20] H. Akagi, E. H. Watanabe, and M. Aredes, "Instantaneous power theory and applications to power conditioning." New York: IEEE Wiley, 2007.

[21] X. Guo, W. Wu, and Z. Chen, "Multiple-complex coefficient-filter-based phase-locked loop and

synchronization technique for three-phase grid-interfaced converters in distributed utility networks," *IEEE Trans. Ind. Electron.*, vol. 58, no. 4, pp. 1194–1204, Apr. 2011.